

# Exergoeconomic and exergoenvironmental analysis of an integrated solar gas turbine/combined cycle power plant

Giuseppe Bonforte <sup>a</sup>, Jens Buchgeister <sup>b</sup>, Giampaolo Manfrida <sup>a</sup>, Karolina Petela <sup>c,\*</sup>

<sup>a</sup> Università degli Studi di Firenze, Department of Industrial Engineering, Viale G.B. Morgagni 40, Firenze, 50134, Italy

<sup>b</sup> Institute of Engineering Thermodynamics, German Aerospace Center, Pfaffenwaldring 38–40, Stuttgart, 70569, Germany

<sup>c</sup> Silesian University of Technology, Institute of Thermal Technology, Konarskiego 22, Gliwice, 44-100, Poland

## ARTICLE INFO

### Article history:

Available online 12 May 2018

### Keywords:

Combined-cycle power plants

Solar thermal integration

Economics

Exergoenvironmental analysis

Life cycle analysis

## ABSTRACT

Integration of solar power to Combined Cycle Power Plants is a solution attracting increasing interest, bridging solar thermal technology to a well-proven energy conversion solution. The integration is attractive for countries aiming to pass to natural gas as an energy feedstock and it could improve the environmental performance. In order to identify the performance and potential environmental benefits, a model of the plant was applied. It covered an annual operation period and included the effects of surroundings variables. The model allows to predict the power plant performance, and calculates a complete exergy balance for all the components of the complex plant. The calculations are repeated for referential CCGT and for the Integrated Solar CCGT.

A complete exergoeconomic and exergoenvironmental model was applied at the design conditions after evaluating the cost of equipment and their environmental score using a detailed Life Cycle Assessment (LCA) modelling tool. The results, applied to a power plant in Southern Poland, show that the solution can be attractive for improving the environmental performance of a CCGT (CO<sub>2</sub> emission factor decreased by 9%), and that the capital cost is only slightly increased so that the rate of return of the investment is only marginally affected.

© 2018 Elsevier Ltd. All rights reserved.

## 1. Introduction

One of the greatest challenges of the 21st Century is to provide a dependable energy supply, limiting climate change issues connected to greenhouse gas emissions and considering economic aspects which are necessary for a sustainable development. Therefore, the future requirement for the design of energy conversion systems is to reduce environmental impacts with limited drawbacks on costs.

For this purpose, the integration of solar power into existing or foreseen Combined Cycle Gas Turbine (CCGT) power plants is a solution attracting increasing interest, bridging solar thermal technology - presently, an expensive alternative when implemented alone - to a well-proven and developed energy conversion solution. Present study focuses on hybridized plants employing Concentrated Solar Power (CSP) technologies.

The concept of the integration of combined cycle and

concentrating solar power plants - first proposed in the 90s by Luz Solar International [1], the builders of the SEGS trough plants in California [2] - has been applied in the power generation sector to help reduce the costs of solar energy for electricity generation. Nowadays, several ISCCs are operating in North Africa [2–5], Middle East [6], Southern Europe [7] and United States [8] and other plants are planned in California [9] and Kuwait [10].

The integration appears to be particularly attractive for countries passing to natural gas as major energy feedstock, and it can reduce the environmental burden associated to the use of fossil fuels. This form of hybridization takes advantage of existing infrastructure at a conventional thermal power plant, including power transmission links to the grid and availability of space around the power plant. Nevertheless, in addition to the supplementary expense for their construction and operation, integrated solar power plants imply some environmental drawbacks in terms of land occupation, use of metal-based raw materials and possibly intensive high-technology fabrication processes.

In the face of numerous profits but also awareness of the weak points, the technology has become a topic of many research works dealing with optimization issues. In one of the latest papers [11]

\* Corresponding author.

E-mail address: [karolina.petela@polsl.pl](mailto:karolina.petela@polsl.pl) (K. Petela).

researchers studied the optimal choice of concentrated solar technology (linear Fresnel collectors, parabolic trough collectors, solar tower) to be integrated with combined cycle power plant. They concluded that the highest radiation-to-electricity efficiency is obtained if parabolic trough collectors are added to the bottoming part of the cycle. In Ref. [12] researchers were looking for optimal control parameters under practical time-dependent constraints of an integrated solar combined cycle power plant. By changing three operational variables (turbine part load indicator, solar focus rate, solar heat transfer fluid mass flow rate, the optimization algorithm was considering multiple different objective functions: maximization of electric output, maximization of profit, maintaining the outlet heat transfer fluid temperature. The results revealed that the system mostly profits from variable heat transfer fluid flow rate conditions.

Here presented paper is aimed to add a different, although already defined, touchstone for further optimization ideas. A comprehensive evaluation of thermodynamic, economic and environmental aspects will always be necessary to understand benefits and limitations of this technology. A useful parameter to investigate these three aspects of an energy conversion system is exergy. It is understood as the only rational basis for assigning monetary and environmental-impact values to the transport of energy and to thermodynamic inefficiencies within the components.

The cost analysis can be carried out applying the concept of exergoeconomic analysis which combines exergy and economics principles. This method has been widely applied for the analysis of conventional thermal power plants [13] and became a useful tool for the thermoeconomic study of ISCCs plants [14,15]. The researchers in Ref. [16] analysed a combined cycle integrated with parabolic trough collectors. Their aim was to minimize the equipment investment cost and cost of exergy destruction. The first objective is governed by economic constraints, the second by thermodynamic requirements. The sensitivity analysis showed that the unit cost of electricity could be reduced by 14% if solar field operation periods were increased from 1000 to 2000.

However, low cost requirement for electrical power generation should be simultaneously combined with a low environmental impact. The exergoenvironmental analysis, a combination of an environmental assessment and exergy analysis, is applied to assess this second aspect. This methodology has been developed for different energy conversion systems [13,17–19] but there is only a unique application for ISCC plants [20]. The author in Ref. [20] analyses a 400 MW ISCC where the solar fields support only high pressure part of the HRSG. According to the findings, addition of solar field may help reduce the environmental impact per exergy unit of electricity by 3.8%

Therefore, there is still an explicit lack of studies on ISCCs that combine thermoeconomic and thermoenviromental approaches supporting decision-makers with meaningful information from economic and environmental point of view at the same time. Additionally, there is a lack of research about the advantages and drawbacks of ISCCs located in regions where the solar radiation is not so favourable. This study is unique for this application.

The purpose of this work is to analyse the exergoeconomic and exergoenvironmental effects and possible improvements of advanced integration between combined cycle power plant and solar thermal energy conversion system. The analysis relies on comparison between a conventional combined cycle gas turbine and an integrated solar combined cycle gas turbine, both applied to the reference case of a power plant in Southern Poland. A model of the plant was developed covering a one-year operation period and including the effects of climatic variables (complete simulation of the solar resource profile, and off-design effects for the gas turbine

performance). The model can predict the power plant performance, and calculates a complete exergy balance including all the components of the plant in both cases.

## 2. Plant configuration description

### 2.1. Reference plant

A power plant under construction in Stalowa Wola, Poland, is the reference case and the starting point for the following solar energy integration study. The system under investigation is a CCGT with a three-pressure level Heat Recovery Steam Generator (HRSG). A model of the CCGT was preliminary built with the use of Equation Solver Modular System (ESMS), a simulation tool developed for complex power plant simulations [21]. The power plant is equipped with the 9F.05 gas turbine produced by General Electric – a 50 Hz heavy-duty gas turbine with a design power output of 299 MW [22]. The steam turbine MTD60, delivered by Škoda Power is a condensing turbine with a double reheat system equipped with bleedings for possible extraction of process steam at pressure of 6 bar, producing maximally 240 MWt of heat [23]. The mathematical model of the three-pressure HRSG and of the steam plant island follows the scheme represented in Fig. 1. The cycle layout machine has double-casing turbines with combined high-intermediate pressure sections and double flow in the low-pressure section; steam reheating at the intermediate pressure level is included.

The modelling approach requires the definition of specific temperature differences between flue gases and water inside the HRSG. The design-point analysis indicated that it is possible to produce 288 MWe by the gas turbine and 152 MWe by the steam turbines with a 57.9% overall plant electric efficiency. After sizing the heat exchangers, it was possible to perform also an annual off design analysis, where the ambient conditions affect gas turbine performance. A detailed description of the reference design data assumed and results in terms of flow rates, energy and exergy can be found in Ref. [24].

### 2.2. The solar integration

Solar thermal hybridization is in principle an advantageous improvement, basing on the addition of a solar heat generating field to an already existing fossil fuel power plant. However, the scope of the integration must be clearly defined. The idea of integration presented in this study is to reduce the bottle-necks of the evaporation process by adding solar heat in parallel. Three groups of solar collectors assembled in solar fields support evaporators operating inside the HRSG (see Fig. 2 for a concept layout). The solar integration is designed taking care that the addition of supplementary heat to evaporators from a parallel solar heat exchanger

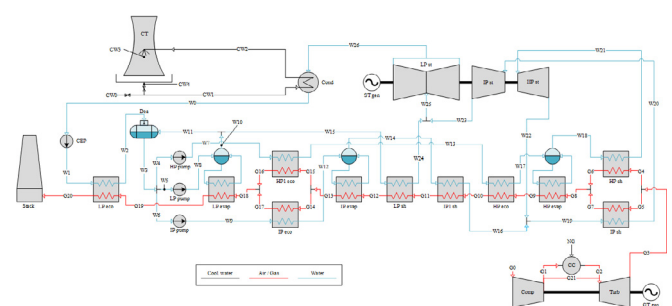


Fig. 1. Combined Cycle Gas Turbine layout.

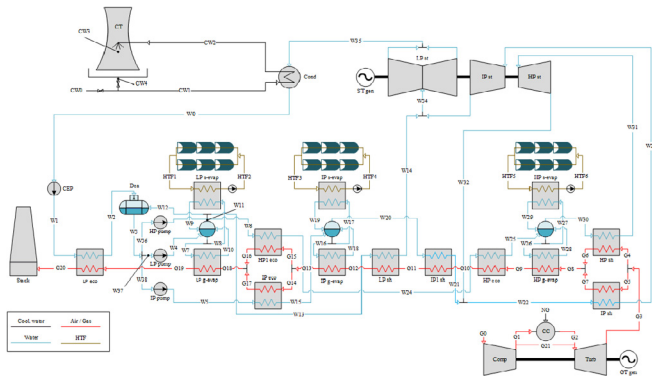


Fig. 2. Integrated Solar Combined Cycle Gas Turbine concept layout.

contributes to diminishing the local temperature difference between the water/steam and gas streams in the HRSG; this increases the power plant energy efficiency through the boost of the steam cycle power output, resulting from the extended heat recovered in the HRSG; consequently, it determines a decrease of the stack temperature. Thereby, the solution here proposed produces both a fuel saving (substituting fuel with solar integration) and a power boosting effect (due to solar integration and improvement of exhaust gas recovery).

The Integrated Solar Combined Cycle Gas Turbine (ISCCGT) plant model demands the definition of the design (solar-provided) heat rates supporting each level of evaporation. The detailed methodology is described in Ref. [20]. The useful heat gain from each solar collector loop was calculated multiplying the solar collector efficiency by the solar radiation reaching the collector surface. The solar collector model is based on the 2-nd order Bliss Equation [25]:

$$\eta_{SC} = \eta_0 - a_1 \frac{\Delta T_m}{G} - a_2 \frac{\Delta T_m^2}{G} \quad (7)$$

Where

$$\Delta T_m = T_{HTF} - T_{amb} \quad (8)$$

The efficiency parameters were provided by manufacturers. The objective was to find a solar collector type that will assure obtaining the saturation conditions (139 °C for low pressure level 3.5 bar; 232 °C for intermediate pressure level 29.2 bar, 329 °C corresponding to high pressure 126.5 bar). The LP evaporator is supported by a solar field using *PolyTrough* 1800 collectors with *NEP SOLAR AG* [26]. For the high and intermediate HRSG pressure levels *EuroTrough* collectors *ET-150* [27] are considered with *SYLTHERM 800* as heat transfer fluid [28]. *PolyTrough* solar collector allows to reach lower outlet temperatures (max. 230 °C) than the *EuroTrough* which is sufficient for the low pressure saturation conditions and were chosen as better suited for the LP field. The whole year simulation of solar collectors revealed that the design morning hour of 17th July provided one of the highest useful heat gain output from the collectors, with an ambient temperature close to ISO standards (16.7 °C). The scale of evaporator support and the size of solar fields were defined for this design condition. A satisfactory level of the design heat duties of the solar back-up evaporators was found performing a sensitivity analysis. Assuming that the lower saturation temperature of low and intermediate pressure levels are easier to be obtained, the idea was to find configuration substituting those 2 evaporators. But yet, it occurred to be impossible. Basing on the multi-variant analysis: if supplementary heat was added at every pressure stage to evaporators, at one point a

phenomenon of heating flue gases in the intermediate pressure evaporator would always appear. Therefore, it has been decided that the final configuration will ensure the lowest heat transfer from flue gases to water in evaporators with the limitation of minimum 3 K pinch point temperature increase. The integration should assure an effective decrease of stack temperature of more than 5 K. Consequently, 40, 20 and 70 MW of thermal energy should be provided by the solar fields at the low, intermediate and high-pressure evaporator levels, respectively. The feasibility has been checked together with the maximum operational parameters of applied steam turbine model [23].

An innovative concept applied to this solar integration case is the arrangement of the collector loops for the high and intermediate pressure evaporators collectors as a flexible (dynamic) solar field. Firstly, following good practice in solar thermal energy conversion systems, a solar multiplication factor  $SF = 1.5$  was applied. The configuration and number of loops dedicated to the intermediate or high-pressure evaporators can be adapted by a simple collector switching arrangement to the meteorological conditions, with priority given to intermediate pressure solar field as less demanding and capable of operating at higher efficiency (because of the lower absorber temperature). Additionally, the solar collector control mode was enhanced implementing a control routine determining the correct increase of HTF temperature. Rather than setting  $\Delta T_{HTF}$  as a fixed value, its value is dynamically adapted according to the radiation and environmental conditions. The fundamental idea of this control law is to maximize the exergy increase in the collector [29].

In order to be able to judge the quality of the integration, main parameters resulting from thermodynamic analysis of the plants are presented in Table 1.

Table 1

Exemplary parameters resulting from the thermodynamic analyses.

Parameter	CCGT	ISCCGT
Gas turbine power output [kW]	288881	288881
Steam turbine power output [kW]	151817	194053
Power plant electrical efficiency [%]	57.9	63.3
Exhaust temperature at the stack - G20 [K]	367.7	360.5
Steam temperature at the HP steam turbine inlet - W31 [K]	815.6	768.55
Steam temperature at the IP steam turbine inlet - W23 [K]	815.6	773.96
Steam temperature at the LP steam turbine inlet - W34 [K]	553	523
Generator electrical efficiency [%]	98.6	98.6

### 3. Methodology

To identify the advantages of technical performance, costs and environmental benefits, a comparison between the conventional configuration and the integrated solar layout was carried out.

As shown in Fig. 3, the concept of exergoeconomic and exergoenvironmental analysis consists mainly of the following three steps:

- Exergy analysis of the investigated system;
- Total revenue requirement cost analysis and Life Cycle Assessment (LCA) of each system component and system input flow;
- Assignment of costs (exergoeconomic analysis) and environmental impacts (exergoenvironmental analysis) to each exergy flow.

The results are critically reviewed in the light of evidencing the advantages of solar integration, and of proposing possible improvements to the design configuration.

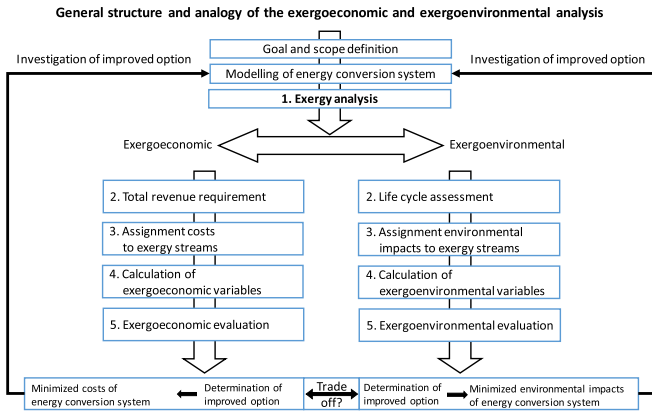


Fig. 3. Exergy, exergoeconomic and exergoenvironmental analysis – General structure, steps and analogies [30].

### 3.1. Exergy analysis

For exergy analysis, first, the boundaries of the system and the components involved must be defined. All relevant system sub-units that have a productive purpose should be regarded as separate components to provide the highest possible level of detail [31]. Next, the exergy values of all material and energy flows within the system must be determined. In exergy analysis, the  $k$ -th component is characterized by the definition of its exergy of product,  $\dot{E}_{P,k}$  and exergy of fuel  $\dot{E}_{F,k}$  shown in Fig. 4.

$$\dot{E}_{F,k} = \dot{E}_{P,k} + \dot{E}_{D,k} \quad (1)$$

$$\dot{E}_{F,tot} = \dot{E}_{P,tot} + \dot{E}_{D,tot} + \dot{E}_{L,tot} \quad (2)$$

The exergy destruction  $\dot{E}_{D,k}$  in the  $k$ -th component is a direct measure of its thermodynamic inefficiency and can be calculated by (1). The exergy analysis provides answers to where thermodynamic inefficiencies occur in the system and allows a fair comparison of irreversibilities of different nature in a complex power plant.

### 3.2. Exergoeconomic analysis

Exergoeconomic analysis combines an exergy analysis of the energy conversion system followed by an economic analysis based on the method of total revenue requirements (TRR), which considers the entire life cycle of the energy conversion system. At the beginning, the total capital investment is calculated according to [32] and [33]; then, based on assumptions for economic, financial, operating, and market input parameters, the yearly total revenue required is computed. This TRR value represents the production cost of the system products, and compensates all the expenditures incurred each year of the project economic life to guarantee an economic plant operation. Afterwards, the yearly variable product

costs associated with the investment, operating, maintenance, fuel supply, and other expenses (cost categories) are levelized. These means are converted to an equivalent series of constant payments called annuities. In the next step, the costs are assigned to the corresponding exergy flows by calculating the specific cost rate of each material and energy flow.

### 3.3. Exergoenvironmental analysis

The procedure for exergoenvironmental analysis is analogous to that of the exergoeconomic analysis. The exergoenvironmental analysis combines an exergy analysis of the energy conversion system with an environmental analysis based on the LCA method, which considers the entire life cycle of the system and determines the environmental impacts. The LCA is applied to assess the environmental impact of the considered system over its lifetime. This methodology is internationally accepted and follows the guidelines of ISO 14004. The Life Cycle Inventory necessary to complete the study is based on [34] and [35]. Assuming a linear dependency between the required material per power unit and the total power output, it is possible to estimate the total mass of the power plant.

Next, these are propagated by the exergy flows in the process. Then exergoenvironmental variables are calculated to enable the analysis. At the development of the exergoenvironmental analysis, the ReCiPe method (further development of Eco-Indicator 99 method) was applied to calculate the environmental impacts for life cycle impact assessment [36].

The results of the LCA (expressed in ReCiPe points) are assigned to the corresponding exergy flows by calculating the specific environmental impact rate of each material and energy flow  $b_j$  (expressed in ReCiPe points per exergy unit). The latter depends on the environmental impact rate  $\dot{B}_j$  and the exergy rate  $\dot{E}_j$  of the  $j$ -th stream:

$$b_j = \frac{\dot{B}_j}{\dot{E}_j} \quad (3)$$

The environmental impacts associated with the supply of an input stream (e.g. the impacts of extraction, transport and conditioning of natural gas) can be calculated directly. To calculate the values for internal streams as well as for output flows, the functional relations among the system components have to be considered. This is done by formulating environmental impact balances for all components  $k$  of the system:

$$\sum \dot{B}_{j,k,in} + \dot{Y}_k = \sum \dot{B}_{j,k,out} \quad (4)$$

Basically, all environmental impacts entering a component have to exit the component associated with all output flows. Therefore, there is not only an exergy flow through the system but also a flow of environmental impacts. Besides the environmental impacts associated with incoming exergy flows, also component-related environmental impacts  $\dot{Y}_k$  associated with the  $k$ -th component

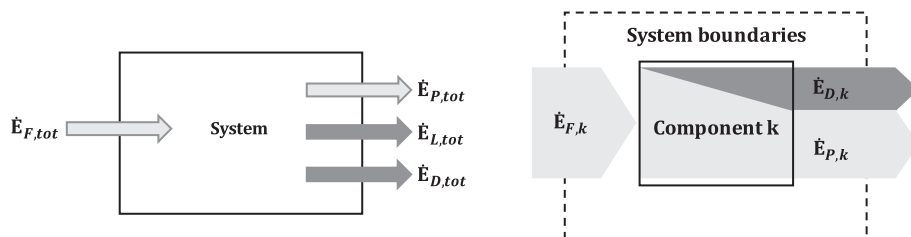


Fig. 4. Basic exergy balance for the total system and for component  $k$ .



**Table 2**

Main equations for exergoeconomic and exergoenvironmental analyses.

Exergoeconomic Analysis	Exergoenvironmental Analysis
Exergy stream cost rate: $\dot{C}_j = c_j \cdot \dot{E}_j$	Exergoenvironmental stream impact rate: $\dot{B}_j = b_j \cdot \dot{E}_j$
Component cost balance: $\sum \dot{C}_{j,k,in} + \dot{Z}_k = \sum \dot{C}_{j,k,out}$	Component environmental impact balance: $\sum \dot{B}_{j,k,in} + \dot{Y}_k = \sum \dot{B}_{j,k,out}$
Component-related cost rate: $\dot{Z}_k = \dot{Y}_K^{CI} + \dot{Y}_K^{OM}$	Component-related environmental impact rate: $\dot{Y}_k = \dot{Y}_K^{CO} + \dot{Y}_K^{OM} + \dot{Y}_K^{DI}$
Component relative cost difference: $r_k = \frac{c_{p,k} + c_{f,k}}{c_{f,k}}$	Component relative environmental impact difference: $r_{b,k} = \frac{b_{p,k} - b_{f,k}}{b_{f,k}}$
Component exergoeconomic factor: $f_k = \frac{\dot{Z}_k}{\dot{Z}_k + \dot{C}_{D,k}}$	Component exergoenvironmental factor: $f_{b,k} = \frac{\dot{Y}_k}{\dot{Y}_k + \dot{B}_{D,k}}$

are considered.

The environmental impacts that occur during the three life cycle phases construction  $\dot{Y}_K^{CO}$ , operation and maintenance  $\dot{Y}_K^{OM}$  and disposal  $\dot{Y}_K^{DI}$  constitute the component-related environmental impacts and are obtained by LCA:

$$\dot{Y}_k = \dot{Y}_K^{CO} + \dot{Y}_K^{OM} + \dot{Y}_K^{DI} \quad (5)$$

On the basis of the exergy and environmental impact rates and the specific environmental impacts of each exergy stream in the process, the exergoenvironmental variables can be calculated for every process component. Of specific interest is the environmental impact rate  $\dot{B}_{D,k}$  associated with the exergy destruction  $\dot{E}_{D,k}$  in the  $k$ -th component, which is calculated by applying the following equation, being based on established rules for the definition of exergetic fuel and product [37]:

$$\dot{B}_{D,k} = b_{f,k} \cdot \dot{E}_{D,k} \quad (6)$$

The exergy destruction rate is multiplied by average specific environmental impacts of the exergetic fuel of the  $k$ -th component  $b_{f,k}$ .

Analogous formulas for exergoeconomic and exergoenvironmental analyses are presented in Table 2.

## 4. Results

For the ISCCGT, the design hour simulation indicated that the steam power output can be increased to 194 MWe and the power plant electric efficiency can reach 63.45%. The energy efficiency of the ISCCGT is calculated with a marginal approach, that is, assuming that only natural gas contributes to the energy input. Hence, the marginal electrical efficiency is raised more than 5% points. The CO<sub>2</sub> emission factor is decreased from 346 gCO<sub>2</sub>-Eq/kWh to 315 gCO<sub>2</sub>-Eq/kWh. The exhaust gas temperature at the stack is reduced from 367.7 K to 360.5 K [24], thereby proving that the hybridization process is effective and reaches its design goals. Subsequent exergy analysis revealed which components induced highest exergy destruction or loss rate. Preliminary exergy analysis indicates that for both systems the combustion chamber incurs the most significant exergy destruction. This result is attributable to the significant irreversibilities associated with the chemical reaction and heat transfer across the large temperature differences between the gas burners and the working fluid. It may seem that increase in

inlet and outlet temperatures reduces the values of the exergy destruction rate. However, an increase in the outlet temperature of the CC causes not only an increase in its efficiency but it also results in an increment of the exergy destruction rate associated with the gas turbine. Only an advanced exergy analysis of endogenous and exogenous destructions may answer this doubt.

On the other hand, the highest relative exergy losses in the conventional power plant are related to the unavoidable stack-loss (80%), while in the ISCCGT solar collector components are causing 90% of relative exergy loss. It results from the subsequent exergoeconomic analysis that this component is also evidently changing the cost indicators (see Fig. 5).

### 4.1. Results - exergoeconomic analysis

The Exergoeconomic Analysis is run for the design operating conditions and the results refer to USD currency. The results show that the cost of exergy destruction in the combustion chamber is dominant for both power plant configurations (see Fig. 5), on account of the high irreversibility of the combustion process. Improvement of this term depends on materials and cooling techniques applied, and on the gas turbine pressure ratio.

The impact of hybridization on the Power Plant Capital Costs is relevant, as is shown in Table 3. However, the economic balance is dominated by the cost of natural gas, so that a substantially higher capital cost exposure can be well motivated (the economic payback return time being about 5 years).

Considering the ISCCGT plant, a large component-related cost (indeed the second contribution in overall relative terms) is associated with the solar collectors. The capital + O&M cost for the three solar fields represents more than 40% of the overall power plant investment costs. Parabolic trough solar technology is the most proven solar power technology; however, the capital cost of the solar collector fields represents a major add-on with respect to that of the conventional combined cycle. This is an important limit

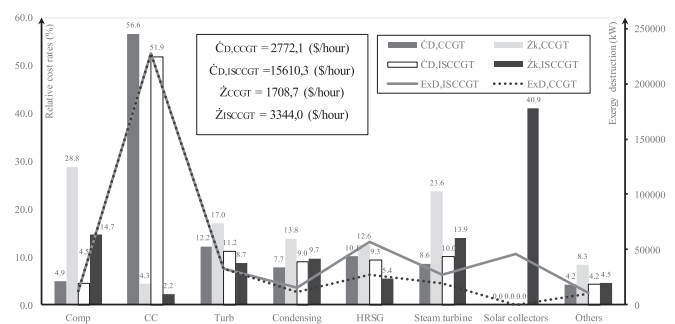


**Fig. 5.** Relative exergy destruction and component-related cost rates.

**Table 3**

Specific capital cost for the two different power plant configurations (\$/kW).

Component	ISCCGT	CCGT
HRSG	121	101
Gas turbine	366	401
Steam turbine	199	188
Condensing system	139	111
Solar collectors	395	0
Others	62	67
<b>Total</b>	<b>1282</b>	<b>867</b>
Fixed O&M [\$ /kW-y] ([\$/kWh])	20.73(0.0026)	13.80(0.002)
Fuel Cost [\$/kWh]	0.0628	0.0633

for the large commercial-scale development of CSP technology; however, ISCCGT power plants represent a bridging technology with respect to solar-only power plants of similar size, because solar energy represents on the whole a marginal support to the HRSG, substituting partially natural gas and improving – in the present case – the flue gas heat recovery process. In terms of fuel cost, since that of solar energy is assumed to be zero, the resulting cost of exergy destruction for the collectors is accounted as 0 \$/hour.

Other meaningful components to the cost build-up are the condenser, HP evaporator, HP super-heater and steam turbine for both CCGT and ISCCGT. The low values of related  $f_k$  suggest that a decrease in cost rate of exergy destruction of these components is possible by a higher investment cost. This solution would lead to an improvement of the system performance.

#### 4.2. Results – exergoenvironmental analysis

Following the results of the LCA inventory, the major contributions to the system-related environmental impact rate come from those components construction requiring significant amounts of metals for construction, such as generators, HRSG and steam turbine. When considering the ISCCGT configuration, the construction of the solar fields is dominant within the system-related environmental impact rate. However, this contribution is not comparable to that of the combustion chamber, since the environmental burden of the gas turbine emissions is completely allocated to this component (see Fig. 6).

Despite the increase in  $\dot{Y}_{tot}$ , the specific environmental impact per unit of energy produced by the integrated solar power plant (38.9 Pts/kWh) is lower than that of the conventional combined cycle (40.2 Pts/kWh). Further insight can be gained re-interpreting the impact with traditional LCA methodology. Fig. 7 presents the main reductions of the specific impact achievable by solar integration sorted by category and referred to the functional unit (1 kWh). Some of them, such as land occupation and metal depletion, have negative values. In particular, the metal depletion for the ISCCGT is higher than that of the CCGT due to the materials stock needed for the construction of the solar fields. The most significant savings are linked to climate change and to depletion of fossil fuels.

This result is confirmed by the carbon footprint, whose profile is resumed in terms of a return payback analysis, presented in Fig. 8. The hybrid power plant, thanks to its diminished consumption of natural gas has a lower CO<sub>2</sub>-Eq. emission per kWh of energy. This fact leads to an important reduction of CO<sub>2</sub>-Eq. emissions throughout the lifetime of the power plant.

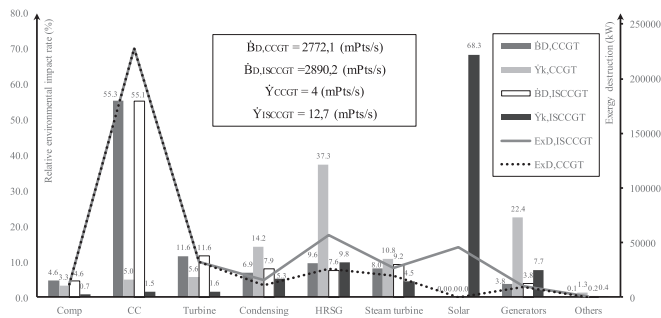


Fig. 6. Relative exergy destruction and component-related environmental impact rates.

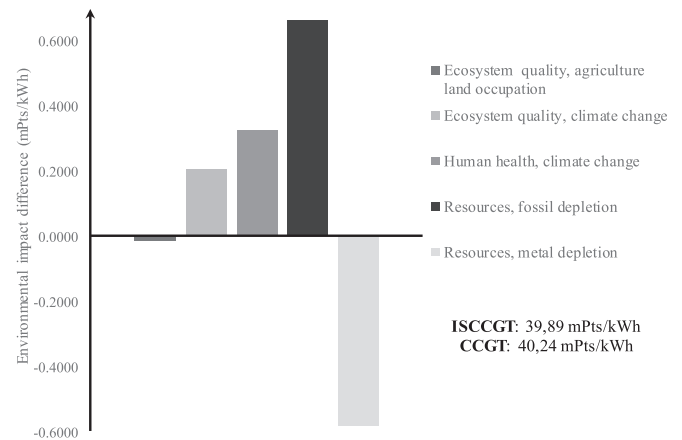


Fig. 7. Environmental impact reduction by ReCiPe impact category.

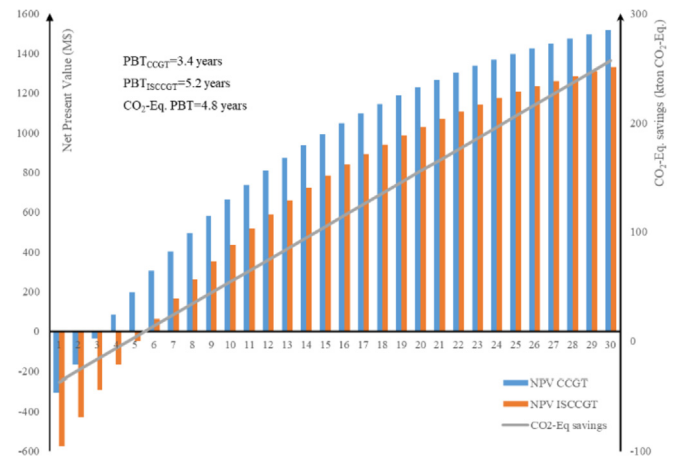


Fig. 8. Lifetime CO<sub>2</sub>-Equivalent emissions analysis.

#### 4.3. Sensitivity analysis

In order to quantify the influence of chosen input parameters on outputs connected with exergoenvironmental and exergoeconomic indicators, a sensitivity analysis has been conducted. In the comprehensive analysis it has been tested how the change of assumed plant lifetime, heat exchangers efficiencies, unit component costs and unit environmental impact rate of a component could affect e.g. product stream cost rate ( $\dot{C}_{p,tot}$ ), total exergy cost rate ( $\dot{Z}_{tot}$ ), exergoenvironmental impact rate of the product stream ( $\dot{B}_{p,tot}$ ) or total environmental impact rate ( $\dot{Y}_{tot}$ ). The subscript *tot* refers to the whole power plant balance.

Fig. 9 presents how the before-mentioned indicators would have behaved, if the plant lifetime had changed. To show the magnitude of change – corresponding cost rates and exergoenvironmental impact rates were divided by their reference value if 30 years are considered.

It is revealed that the component related total exergy cost rate and total environmental impact rate are most intensively affected by this change: it is visible that if plant lifetime had been decreased 6 times,  $\dot{Z}_{tot}$  and  $\dot{Y}_{tot}$  would have been 6 times higher. On the other hand, the sensitivity of stream related exergy cost rate to plant lifetime modification is less visible: if it was 10 instead of 30 years, this indicator would be only 20% higher. In the meantime, the exergoenvironmental impact rate of the product stream ( $\dot{B}_{p,tot}$ ) would remain unchanged.

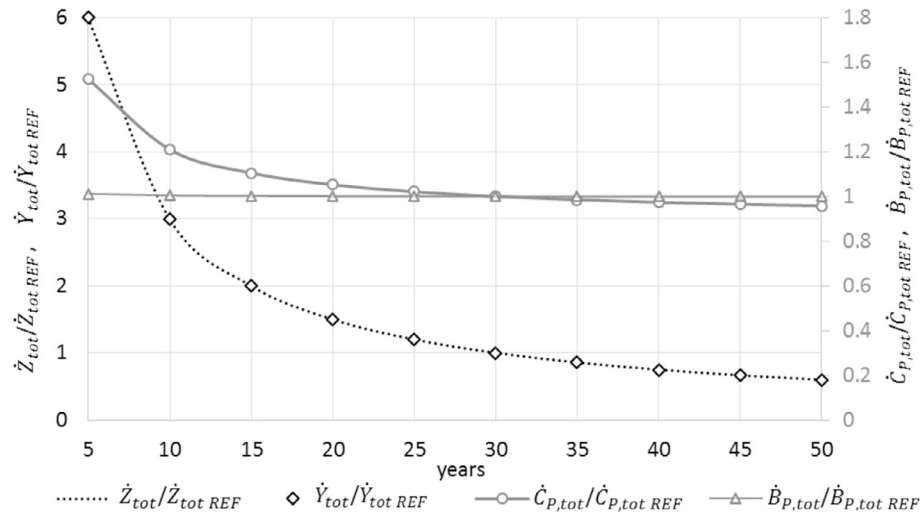


Fig. 9. Sensitivity of exergoeconomic and exergoenvironmental impact rates to the assumed plant lifetime.

Fig. 10 presents dependence of product stream exergy cost rate on the potential change of solar collector efficiency. Its influence is limited: averagely, if collector efficiency was increased by 20%, the product stream exergy cost rate would have risen by 1%. Although the effect is hardly visible, one can notice that the steepest curve refers to the efficiency of solar collectors supporting HP evaporator. It is understandable, since these collectors provide the highest additional heat input at the highest temperature level contributing to collector efficiency reduction.

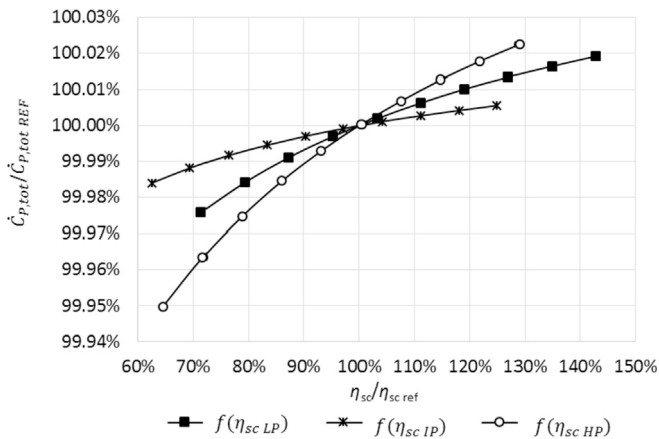


Fig. 10. Sensitivity of product stream cost rate ( $\dot{C}_{P,tot}$ ) to the change of solar collector efficiency.

## 5. Conclusions

The present work investigates the economic and environmental performance of an ISCCGT and compares it with that of the correspondent conventional CCGT by a detailed exergoeconomic and exergoenvironmental analysis.

Specifically, the ISCCGT hybridization was aimed to improve heat recovery in the HRSG, reducing pinch problems and achieving a lower stack temperature; moreover, a dynamic allocation of the CSP solar fields supporting the mid- and high-pressure evaporators, and flow rate control minimizing the solar collectors exergy destruction and loss are applied, providing notable results for the

year-round off-design operation of the plant.

The capital cost is increased about 48% by solar hybridization, but the rate of return of the investment (5.2 years) is only marginally affected because of the combined effect of saving the expensive natural gas resource and power boosting. The revenue resulting from the conventional CCGT has a higher dependency on the NG price while the ISCCGT, thanks to its lower request of heat per unit of energy produced can better face eventual increases in the fuel cost. In addition, it should be considered that the power plant is located in a region that does not offer an optimal solar irradiation. The solar field surface, and so the investment cost, is then larger than required in areas with better climate conditions.

The exergoeconomic and exergoenvironmental analyses, including a detailed LCA, were applied to the design operating conditions. The results confirm that, despite a higher  $\dot{Y}_{tot}$ , the ISCCGT technology offers significant environmental advantages thanks to its lower consumption of fossil fuel per unit of produced energy, with consequent reduction of greenhouse gases emissions throughout the operational lifetime. Possible design modifications mentioned to improve the exergoeconomic and exergoenvironmental indicators include: potential change of gas turbine materials and cooling technique, use of less expensive solar collectors (available high temperature flat plate collectors, applicable also for intermediate pressure level), verification of applied solar multiplication factor significantly contributing to the cost rates and cumulative environmental impact, limitation of solar integration only to IP and HP evaporators. Eventually, change of plant location to more favourable meteorological conditions would also have a positive reflection on the exergoeconomic analysis results. Nevertheless, analyzing potential benefits resulting from components design modification, one should be aware that reduction of exergy destruction in one component could induce higher irreversibilities in another one and thus lead to higher cost or impact factors. In order to detect this danger, an advanced endogenous and exogenous exergy destruction analysis could be applied.

## References

- [1] Johansson TB, Burnham L. Renewable energy: sources for fuels and electricity. Island Press; 1993.
- [2] Baharoon DA, Rahman HA, Omar WZW, Fadhl SO. Historical development of concentrating solar power technologies to generate clean electricity efficiently – a review. Renew Sustain Energy Rev 2015;41:996–1027. <https://doi.org/10.1016/j.rser.2014.09.008>.
- [3] Concentrating Solar Power Projects - ISCC Hassi R'mel | Concentrating Solar

- Power | NREL [https://www.nrel.gov/csp/solarpaces/project\\_detail.cfm/projectID=44](https://www.nrel.gov/csp/solarpaces/project_detail.cfm/projectID=44). (accessed November 18, 2017).
- [4] Concentrating Solar Power Projects - ISCC Ain Beni Mathar | Concentrating Solar Power | NREL [https://www.nrel.gov/csp/solarpaces/project\\_detail.cfm/projectID=43](https://www.nrel.gov/csp/solarpaces/project_detail.cfm/projectID=43) (accessed November 18, 2017).
- [5] Concentrating Solar Power Projects - ISCC Kuraymat | Concentrating Solar Power | NREL [https://www.nrel.gov/csp/solarpaces/project\\_detail.cfm/projectID=65](https://www.nrel.gov/csp/solarpaces/project_detail.cfm/projectID=65) (accessed November 18, 2017).
- [6] Mapna | YAZD SOLAR THERMAL POWER PLANT <http://mapnagroup.com/en/project/yazd-solar-thermal-power-plant/> (accessed November 18, 2017).
- [7] Archimede Solar Energy [http://www.archimedesolarenergy.it/it\\_reference\\_project\\_1.htm](http://www.archimedesolarenergy.it/it_reference_project_1.htm) (accessed November 18, 2017).
- [8] FPL Solar energy centers: FPL martin next generation clean energy center. 2015. <http://www.renewableenergyworld.com/articles/slideshow/2015/07/fpl-s-martin-next-generation-solar-energy-center.html>. [Accessed 18 November 2017].
- [9] Inland Energy Inc. <http://www.inlandenergy.com/projectv2.html> (accessed November 18, 2017).
- [10] Al Abdaliyah Integrated Solar Combined Cycle (ISCC) | CSP World Map | CSP World <http://cspworld.org/cspworldmap/al-abdaliyah-integrated-solar-combined-cycle-iscc> (accessed November 18, 2017).
- [11] Manente G, Rech S, Lazzaretto A. Optimum choice and placement of concentrating solar power technologies in integrated solar combined cycle systems. *Renew Energy* 2016;96:172–89. <https://doi.org/10.1016/j.renene.2016.04.066>.
- [12] Brodrick PG, Brandt AR, Durlinsky LJ. Operational optimization of an integrated solar combined cycle under practical time-dependent constraints. *Energy* 2017;141:1569–84. <https://doi.org/10.1016/j.energy.2017.11.059>.
- [13] Kumar R. A critical review on energy, exergy, exergoeconomic and economic (4-E) analysis of thermal power plants. *Eng Sci Technol Int J* 2017;20:283–92. <https://doi.org/10.1016/j.jestech.2016.08.018>.
- [14] Bakos GC, Parsa D. Technoeconomic assessment of an integrated solar combined cycle power plant in Greece using line-focus parabolic trough collectors. *Renew Energy* 2013;60:598–603. <https://doi.org/10.1016/j.renene.2013.05.025>.
- [15] Baghernejad A, Yaghoubi M. Multi-objective exergoeconomic optimization of an integrated solar combined cycle system using evolutionary algorithms. *Int J Energy Res* 2011;35:601–15. <https://doi.org/10.1002/er.1715>.
- [16] Baghernejad A, Yaghoubi M. Exergoeconomic analysis and optimization of an integrated solar combined cycle system (ISCCS) using genetic algorithm. *Energy Convers Manag* 2011;52:2193–203. <https://doi.org/10.1016/j.enconman.2010.12.019>.
- [17] Casas-Led On Y, Spauldo F, Arteaga-P Erez LE. Exergoenvironmental analysis of a waste-based Integrated Combined Cycle (WICC) for heat and power production. *J Clean Prod* 2017;164:187–97. <https://doi.org/10.1016/j.jclepro.2017.06.211>.
- [18] Meyer L, Tsatsaronis G, Buchgeister J, Schebek L. Exergoenvironmental analysis for evaluation of the environmental impact of energy conversion systems. *Energy* 2009;34:75–89. <https://doi.org/10.1016/j.energy.2008.07.018>.
- [19] Mergenthaler P, Schinkel AP, Tsatsaronis G. Application of exergoeconomic, exergoenvironmental, and advanced exergy analyses to Carbon Black production. *Energy* 2016;137:898–907. <https://doi.org/10.1016/j.energy.2017.03.107>.
- [20] Cavalcanti EJC. Exergoeconomic and exergoenvironmental analyses of an integrated solar combined cycle system. *Renew Sustain Energy Rev* 2017;67:507–19. <https://doi.org/10.1016/j.rser.2016.09.017>.
- [21] Carcasci C, Facchini B. A numerical method for power plant simulations. *J Energy Resour Technol Trans ASME* 1996;118:36. <https://doi.org/10.1115/1.2792691>.
- [22] Quick and Efficient Solution for Growing Grids [https://st-www.gepower.com/content/dam/gepower-pgdp/global/en\\_US/documents/product/gas\\_turbines/Fact\\_Sheet/9f03-04-05-fact-sheet-april-2015.pdf](https://st-www.gepower.com/content/dam/gepower-pgdp/global/en_US/documents/product/gas_turbines/Fact_Sheet/9f03-04-05-fact-sheet-april-2015.pdf) (accessed November 18, 2017).
- [23] Technical brochure: Products and customer service, Doosan Škoda Power.
- [24] Petela K, Manfrida G, Liszka G, Carcasci C. Integrating solar power in large combined-cycle power plants. In: *Proc. ECOS 2015-28th Int. Conf. Effic. Cost, Optim. Simul. Environ. Impact Energy Syst.*, Pau, ISBN 978-295555390-9. Code 119546.
- [25] Duffie JA, Beckman WA. *Solar engineering of thermal processes*. Hoboken, NJ, USA: John Wiley & Sons, Inc.; 2013. <https://doi.org/10.1002/9781118671603>.
- [26] Technical information: PolyTrough 1800 Technical Specification. Collective work of SPF Institut für Solartechnik ordered by NEP SOLAR AG. Report No.: C1549LPEN.
- [27] Technical information: INABENSA. EUROTROUGH II - Extension, Test and Qualification of EUROTROUGH from 4 to 6 Segments at Plataforma Solar de Almería. *Eur Community* 2002;1–28.
- [28] Technical information: Collective work, Syltherm 800 technical data sheet. the Dow Chemical Company. 2001. Report No.: CH-153-311-E-1101
- [29] Manfrida G, Gerard V. Maximum exergy control of a solar thermal plant equipped with direct steam collectors. *Int J Therm* 2008;11:143–9. <https://doi.org/10.5541/IJOT.1034000222>.
- [30] Meyer L, Castillo R, Buchgeister J, Tsatsaronis G. Application of exergoeconomic and exergoenvironmental analysis to an SOFC system with an allothermal biomass gasifier. *Int J Therm* 2009;12:177–86.
- [31] Bejan A, Tsatsaronis G, George, Moran MJ. *Thermal design and optimization*. Wiley; 1996.
- [32] Roosen P, Uhlenbruck S, Lucas K. Pareto optimization of a combined cycle power system as a decision support tool for trading off investment vs. Operating Costs 2003;42:553–60. [https://doi.org/10.1016/S1290-0729\(03\)00021-8](https://doi.org/10.1016/S1290-0729(03)00021-8).
- [33] Geyer M, Lüpfer E, Osuna R, Esteban A, Schiel W, Schweitzer A, Zarza E, Nava P, Langenkamp J, Mandelberg E. EUROTROUGH - parabolic trough collector developed for cost efficient solar power generation. In: *Presented at 11th Int. Symposium on Concentrating Solar Power and Chemical Energy Technologies*. Zurich; 2002.
- [34] Parthey F. *Lebenszyklusanalyse und Bestimmung von Einflussfaktoren zur nachhaltigen Produkt-gestaltung von GuD-Kraftwerken*. PhD dissertation. 2010.
- [35] Pihl E, Kushnir D, Sandén B, Johnsson F. Material constraints for concentrating solar thermal power. *Energy* 2012;44:944–54. <https://doi.org/10.1016/j.energy.2012.04.057>.
- [36] Goedkoop M, Heijungs R, Huijbregts M, De Schryver A, Struijs J, Van Zelm R. *ReCiPe 2008 first edition (version 1.08) report I: characterisation*. 2013.
- [37] Lazzaretto A, Tsatsaronis G. SPECO: A systematic and general methodology for calculating efficiencies and costs in thermal systems 2006;31:1257–89. <https://doi.org/10.1016/j.energy.2005.03.011>.